forests

MDPI

Article

Assessing the Cooling Effect of Four Urban Parks of Different Sizes in a Temperate Continental Climate Zone: Wroclaw (Poland)

Jan Blachowski * and Monika Hajnrych

Department of Geodesy and Geoinformatics, Faculty of Geoengineering, Mining and Geology, Wrocław University of Science and Technology, Wyb. Wyspiańskiego 27, 50-370 Wrocław, Poland; monika.hajnrych@pwr.edu.pl

* Correspondence: jan.blachowski@pwr.edu.pl

Abstract: Urban parks have been known to form park cooling islands (PCI), which can effectively alleviate the effect of urban heat islands (UHI) in cities. This paper presents results obtained for four different size parks in the city of Wroclaw, which is located in a temperate continental climate. The number of publications for urban areas located in this type of climate and cities is low compared to sites in hot and humid areas. Land surface temperature (LST) maps were developed from Landsat 8 Thermal Infrared Sensor (TIRS) data acquired during three hottest weather periods between 2017 and 2019. Metrics and spatial statistics characterising the four parks selected for the analysis based on their size were calculated. These included: perimeter, area, landscape shape index (LSI) and P_{LC} (forest area) park metrics, and Park Cooling Area (PCA), Park Cooling Efficiency (PCE), Park Cooling Gradient (PCG), Park Cooling Island (PCI) and Extended Park Cooling Island (PCIe) spatial indexes. The averaged PCIe values ranged from 2.0 to 3.6 °C, PCI from 1.9 to 3.6 °C, PCG from 0.7 to 2.2 °C, PCE from 5.3 to 11.5, and PCA from 78.8 to 691.8 ha depending on the park. The cooling distance varied from 110 m to 925 m depending on park size, forest area and land use type in the park's vicinity. The study provides new insight into urban park cooling effects in a medium sized city located in a temperate continental climate, and the role of parks in regulation of urban temperature to mitigate the UHI effect.

Keywords: urban park; forest; cooling effect; spatial analysis; LST; temperate continental climate; Wroclaw; Poland

Citation: Blachowski, J.; Hajnrych, M. Assessing the Cooling Effect of Four Urban Parks of Different Sizes in a Temperate Continental Climate Zone: Wroclaw (Poland). *Forests* **2021**, *12*, 1136. https://doi.org/10.3390/f12081136

Academic Editor: Sandro Strumia

Received: 23 July 2021
Accepted: 17 August 2021
Published: 23 August 2021

1. Introduction

The urban heat island (UHI) effect has become a major issue in modern city management and in urban ecology [1]. The phenomenon, i.e., higher air or surface temperature of urban areas in relation to their surroundings was identified for the first time by Howard in the early 19th Century on the example of the City of London [2]. The reasons for this condition are due to urban surfaces being usually darker than those in the suburban and rural areas (low albedo and reflected sunlight), vegetation cover that in urban areas is typically less than those of surrounding areas, construction materials of buildings, pavements and other urban structures that tend to have high heat rate and store the heat through day hours and emit it during the night, urban morphology which affects shading and air movement, and ever-increasing rates of energy consumption [3–5]. The UHI effect has been aggravated in cities worldwide by climate change and increasing average global temperatures [6,7], as well as by rapid urbanisation and deforestation [8,9]. It has also been proved that UHI effect varies with time of the day (diurnal behaviour) [10,11] and with the season of the year [12,13]. Furthermore, it has been established that UHI influences air pollution dispersion in cities (longer periods of high pollution levels), water usage, higher temperature of ground waters, and bioclimatic conditions adversely affecting health and well-being of their citizens [14–20].

Vegetation is considered to be the most effective method to mitigate the UHI [21,22]. This is because plants reduce impervious surfaces that absorb sunlight and provide shadow, as well as stimulate evapotranspiration that, in combination with shading, can help to reduce high temperatures [23,24]. Vegetation in urban areas can be classified into three main types: street trees, green roofs and walls, and urban parks [5]. The latter urban park is considered to be the most effective way to mitigate the UHI, because a park constitutes an area that combines many types of vegetation including forests, unpaved surfaces and water bodies. Thus, green urban areas can improve resilience of cities to atmospheric and surface urban heat island effects. The effectiveness of green areas, especially parks, in reducing urban heat island has been proven through field measurements, remote sensing and computer simulation [25–30].

An important feature of the UHI are high land surface temperatures (LST). The LST has been widely used, e.g., to analyse change of temperature associated with land use change, urban growth [22,28,31–33] and the urban park cool (or cooling) island (PCI) phenomenon, i.e., lower temperature within a park in relation to its surroundings [34–39].

According to Peng et al. [40] urban park cooling studies can be divided into four types: (1) assessment of park cooling effect [41–43], (2) monitoring of park cooling effect [5,39,44,45], (3) identification of factors influencing park cooling effect [12,37,41,46–48], and (4) design of parks for increased cooling effect [28,30,49,50]. In addition, human thermal comfort assessment studies in parks and their neighbourhood have been conducted [51,52].

Various indexes have been developed or modified to measure the cooling effect of urban parks in the spatial context. These include measures based on the cooling distance, area or intensity, as well as indexes taking into account vegetation or the shape of green area to quantify this effect of urban green spaces (parks) on their surroundings [12]. Research has been conducted from the city (multiple parks) [28,47,50,53,54] to the local (individual park) scales [11,30,38,39,44,51]. Some studies concentrate on nocturnal UHI mitigation [44,55], whereas other ones focus on seasonal changes of this phenomenon [10,45,47,56]. The source data for determining this effect predominately originate from satellite imagery (e.g., Landsat missions) [28,37,40,42,48,57–59] and/or ground measurements using fixed or mobile meteorological stations [5,38,39,51,60–62]. Citizen surveys have been performed to determine the thermal perception and assess the thermal comfort of population in urban parks and their neighbourhood acting as supplementary (qualitative) information for quantitative analyses [51,52,56]. The number of studies concerning the effect of urban green spaces (urban parks) on the UHI has been increasing in recent years. Notable studies related to this research and classified into the type of studies, data and main methods used have been listed in Appendix A, whereas noteworthy examples of early studies include [34,63–65].

Literature review shows that the greatest number of publications focus on large urban agglomerations in Asia, especially in China. The number of studies of urban park cooling effects on the LST in cities located in temperate continental climate zones such as in the case of Poland are limited (Appendix A). Therefore, in our study we examine the cooling effect of urban parks on the example of the city of Wroclaw (SW Poland). We have proposed to select representative parks from four distinct classes basing on park size, and to estimate if the strength of the cooling effect depending on the park characteristics (especially the size and forest area) and the type of land use in park surroundings using selected indexes including one proposed by us.

2. Study Area

The Wroclaw city is located in south-western Poland in Central Europe, on the Silesian Lowland, along the Odra River valley (51°06′36″ N 17°01′20″ E). It is the fourth largest city in Poland in terms of population (643,782 inhabitants in 2020), and the fifth largest city in terms of area (292.82 km sq.) [66]. However, studies show that the real number of people in Wroclaw is estimated to vary between 825 thousand and 1 million [67]. The elevation

of the city area varies from 105 m to 148 m a.s.l., thus the temperature field is practically unaffected by altitude [68].

Wroclaw is located in a moderate, transitional, climate zone subjected to continental and oceanic influences. An important factor affecting the city's climate is its location in the vicinity of areas with varied and elevated topography, i.e., the Trzebnickie Hills in the north, and the Sudetes Foreland and the Sudetes Mountains in the south. The location of the city in the foreground of the Sudetes and in the Odra River valley gives it thermal privilege, known as a Wroclaw area of heat, which is a consequence of the dynamic heating of air masses that settle on the leeward side of the mentioned mountain massif [69].

The city has temperate continental climatic conditions, with a mean annual precipitation of 567 mm. The average air temperature has increased over the past years. In the years 1946–1980 the annual mean temperature was estimated at 8.2 °C [70], in the next two decades (1981–2020) it grew to 9.0 °C [71], and, by 2008–2019 the annual average temperature of Wroclaw was estimated at 10.2 °C, with the coldest month being January (−0.1 °C), and the warmest being July (20.2 °C) [71,72]. Warm and humid weather conditions are common in the Summer; the Winter season is relatively mild with moderate and changeable temperatures [70]. The prevailing wind directions are typically west and south with an average speed of about 2.5 $m \cdot s^{-1}$, according to records collected by the meteorological station located at the Copernicus Airport Wroclaw [73]. The urban heat island phenomenon in Wroclaw has been investigated by Szymanowski and Kryza, who describe its spatial structure as amoebic and multicellular, reflecting the land-use structure of the city [68,74]. The highest temperature zone covers the city centre, connected mainly with dense downtown build-up areas, with the maximum UHI intensity area characterized by the bisection resulting from the existence of the Odra River valley [75]. The annual mean UHI intensity in the centre of the city reaches 1.0 K. It is weaker in Autumn and Winter (0.9 K) than in Spring and Summer (1.1–1.2 K). The magnitude of the night-time UHI is two to three times higher than the average for daytime, as in other cities [74]. The potential factors influencing the local climatic conditions are: transformation of land use cover through housing and technical infrastructure development, emission of pollutants and anthropogenic heat. These processes also influence the occurrence of the urban heat island [70]. Approximately 34% of the Wroclaw city area is built-up, mainly with high-rise buildings and housing estates, industrial and warehouse buildings, as well as transport infrastructure. The urban green spaces account for 34.0%, agriculture for 25.0%, and water for 3.0% of the total area [76]. The urban green area decreased by 2.6 percent points and land used for agriculture by 3.9 percent points in the last two decades. The land use map classified according to the European Union Corine Land Cover Copernicus Land Monitoring Service methodology [77] has been shown in Figure 1.

There are 43 parks and communal forests in Wroclaw with a total area of approximately 527.6 ha. The urban parks vary in shape, size (from 0.57 ha to 78 ha), and type of their surroundings. Location of urban parks within the city limits has been shown in Figure 2.

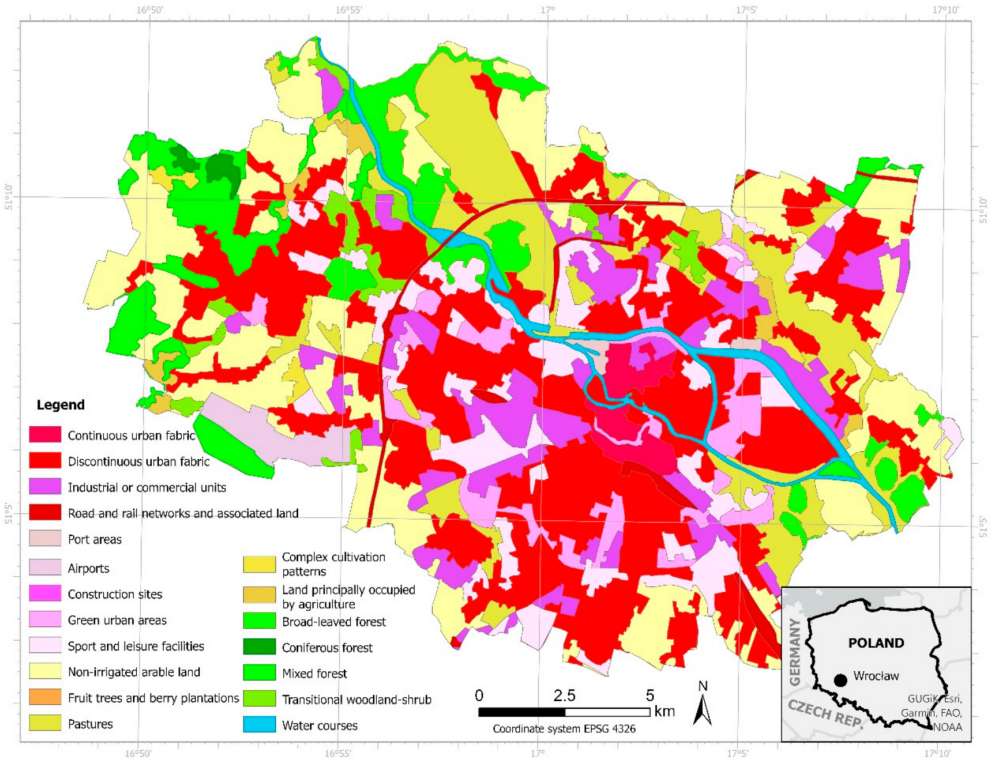

Figure 1. Land use in Wroclaw based on the Corine Land Cover classification (2018).

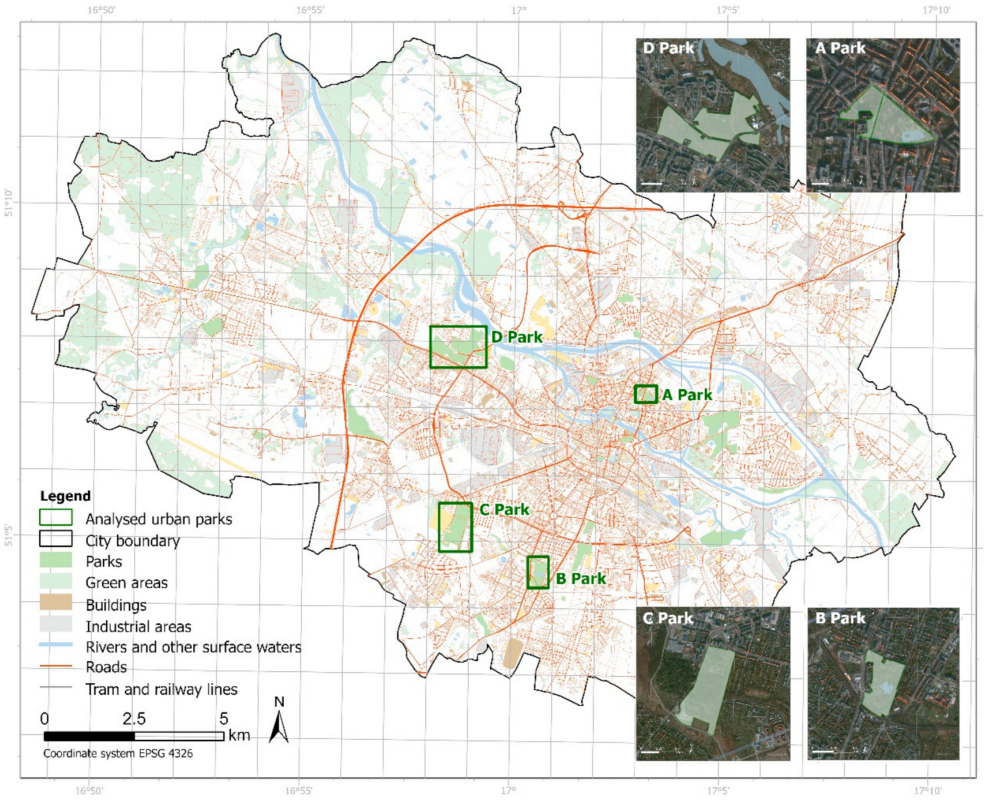

Figure 2. Location of urban parks and built-up area in Wroclaw. Green rectangles indicate case study sites.

3. Data and Methods

3.1. Data Sources

The detailed information on urban parks has been derived from the national Database of Topographical Objects (BDOT10k) that contains information layers representing, among other things, road and railways networks, buildings and installations, land cover and land use, watercourses, and protected areas at a scale of 1:10,000 [78]. To supplement and verify the location and extent of urban parks, an RGB ortomosaic based on aerial images from April 2018 obtained from the Wroclaw Spatial Information System [79] has been used. In addition, the CORINE Land Cover (CLC) inventory representing land use in 44 classes from 2018 [77] has been used to further assess the parks' neighbourhood. The determination of park boundaries have been verified through field reconnaissance.

To obtain a map of the LST in the study area, Landsat 8 Thermal Infrared Sensor (TIRS) images retrieved from the USGS (United States Geological Survey) website [80] and resampled to 30 m have been used. The dates of satellite imagery acquisition have been selected to closely match the hottest periods in Wroclaw, which have been identified through the analysis of historical data from the Wroclaw Airport Meteorological Station. The following cloud free images with a spatial resolution of 30 m have been used in the study (date and time of acquisition, maximum recorded temperature in the city have been given, respectively):

- 28 May 2017, 9:43 GMT, 27.4 °C,
- 3 August 2018, at 9:43 GMT, 32.8 °C,
- 3 June 2019, 9:44 GMT, 28.9 °C.

Geospatial calculations using Map Algebra and cartographic compositions have been conducted in ESRI ArcGIS Pro software [81] licensed to the Wroclaw University of Science and Technology.

3.2. Image Pre-Processing and Retrieval of LST

The Land Surface Temperature (LST) was retrieved from the cloud-free sub-scenes of Landsat 8, path 190 and row 24 obtained from the United States Geological Survey (USGS). The Landsat 8 data acquired by both the Operational Land Imager (OLI) and Thermal Infrared Sensor (TIRS) are delivered in 16-bit unsigned integer format. The LST retrieval followed the procedures described inter alias in [80,82–85].

The Land Surface Temperature (LST) index was calculated using the Landsat-8 thermal bands, band 10 to estimate the brightness temperature and bands 4 and 5 to calculate the Normalized Vegetation Index (NDVI). The process of LST calculation involved the following main steps:

1. calculating the Top of Atmospheric Spectral Radiance,
2. conversion of the Radiance to Sensor Temperature,
3. calculating the NDVI,
4. calculating the Land Surface Emissivity, and
5. LST retrieval.

The first step involved conversion to Top of Atmospheric (TOA) Radiance. The OLI and TIRS bands were used to calculate the spectral luminance (L_λ). At this stage, the values measured by the sensor for each pixel were recalculated using the parameters contained in the satellite image metadata file (MLT file) (1) [80,82–84]:

$$L_\lambda = M_L Q_{cal} + A_L \quad (1)$$

where M_L is the band specific multiplicative scale factor for a given band, A_L is the band specific additive scaling factor and Q_{cal} is the quantized and calibrated standard pixel values of the band 10 product.

The next step included conversion of radiance to radiation temperature (BT). The TIRS data were converted from spectral luminance to radiation temperature. In this step, the radiant temperature unit was corrected, from Kelvin to Celsius degrees (2) [80,82–84]:

$$BT = \frac{K_2}{\ln\left[\left(\frac{K_1}{L_\lambda}\right) + 1\right]} - 237.15 \quad (2)$$

where K_1 and K_2 are the thermal conversion constants characteristic of the given band taken from the metadata file.

Based on the radiation properties of chlorophyll, which strongly absorbs radiation in the near infrared and weakly in the visible range, the Normalized Differential Vegetation Index (NDVI) was calculated following the equation proposed by, e.g., [83,84]. The index enables us to determine the general condition of vegetation, and thus allows for the calculation of the vegetation part (P_v) (3) [80,82–84]:

$$P_v = \left(\frac{NDVI - NDVI_{min}}{NDVI_{max} - NDVI_{min}}\right)^2 \quad (3)$$

To estimate the temperature of the land surface, the emissivity of the surface (ε) was calculated (4) [80,82–84]:

$$\varepsilon = 0.004 \times P_v + 0.986 \quad (4)$$

The final step involved calculation of the emissivity corrected temperature of the land surface (T_s) in Celsius (°C) from (5) [80,82–84]:

$$T_s = \frac{BT}{\left\{1 + \left[\left(\frac{\lambda \times BT}{\rho}\right) \ln_\varepsilon\right]\right\}} \quad (5)$$

where λ is the average wavelength of the emitted radiation and ρ is given by (6) [80,82–84]:

$$\rho = h\frac{c}{\sigma} \quad (6)$$

where h is the Planck's constant (6.626×10^{-34} J s), c is the speed of light (2.998×10^8 m/s) and σ is the Boltzmann constant (1.38×10^{-23} J/K).

3.3. Urban Park Metrics

The landscape metrics are parameters that define specific spatial features for any area [13,86]. In this study, the following metrics were calculated for each of the analysed parks:

1. Park perimeter (P_P),
2. Park area (P_A),
3. Landscape shape index (LSI), which was designed by Patton (1975) and describes the compactness of a patch shape [37], in our case compactness of a park shape (7),

$$LSI = \frac{P_P}{2\sqrt{\pi \times P_A}} \quad (7)$$

The closer the LSI value is to 1.0, the more the shape of the park resembles a circle.

4. Park land cover (P_{LC}) is the structure of a park's land cover types expressed as a percentage of the total park area.

3.4. Spatial Statistics

Spatial statistics provide methods for describing spatial structures and their relationships. These methods allow the analysis of both geographic data and other types of information that have the property of being located in a certain space [87]. In this work, the parks' cooling efficiency was determined in GIS, using the following indexes:

1. Park Cooling Area (PCA), which is the buffer area, formed on the basis of the longest-range distance of the park's influence (the largest cooling distance) [37,40,41].
2. Park Cooling Efficiency (PCE) is the ratio of the maximum cooling area (S_{max}) to the park area (P_A) [37,40] (8):

$$PCE = \frac{S_{max}}{P_A} \quad (8)$$

3. Park Cooling Gradient (PCG), which determines the temperature rise per unit of distance increment (100 m) from the park boundary [11,40,54].
4. Park Cooling Island (PCI), which is the difference between the mean LST outside the park on an urban area (T_U) (in a buffer 500 m from the border) and the mean LST inside the park (T_P) [37,47] (9):

$$PCI = T_U - T_P \quad (9)$$

5. Extended Park Cooling Island (PCIe), which we propose as the difference between the mean LST in the buffer of maximum cooling area (T_R) and the mean LST inside the park (T_P) (10):

$$PCIe = T_R - T_P \quad (10)$$

4. Results

The LST maps for Wroclaw have been used to determine the influence of urban parks on the land surface temperature distribution. The LST maps for selected dates in 2017, 2018 and 2019 have been included in Appendix B. The satellite imagery acquisition dates were selected based on cloud free image availability corresponding to highest recorded daily ambient air temperatures in the city. The highest LST values were observed for 2017 and the lowest for 2018. The basic temperature statistics derived from these maps have been given in Table 1. The mean LSTs for the area of Wroclaw range from 27.6 °C to 28.6 °C. Two maps (for 2017 and 2019) show similar temperature distribution and statistics, with the 2018 one values lower by about 1.0 °C on average. In all the three cases, the obtained spatial distribution of LST corresponds to the spatial structure of UHI in Wroclaw described in [68,71] and presented in the study area section.

Table 1. Basic LST statistics for the area of Wroclaw city.

Value/Year	2017	2018	2019
Min.	19.9 °C	16.0 °C	19.9 °C
Max.	43.9 °C	39.2 °C	43.1 °C
Mean	28.3 °C	27.6 °C	28.6 °C

4.1. Analysis of Urban Park Metrics

The urban parks have been divided into classes depending on the area of each park using the natural breaks classification method. Four distinct classes have been determined with the following value ranges: 0.57–14.78, 21.28–25.11, 37.72–46.22, and 73.44–78.03 ha. The distribution of urban parks sizes has been shown in Figure 3. For the purpose of this study, four representative parks, one from each class, have been selected. The parks have been named: A, B, C and D, where the A Park represents the lowest class and D Park the highest class. In the case of the lowest class, two parks constituting one continuous green area and referred to as A Park (Table 2) were selected for the analysis. The selected parks are located in different parts of the city, as shown in Figure 2.

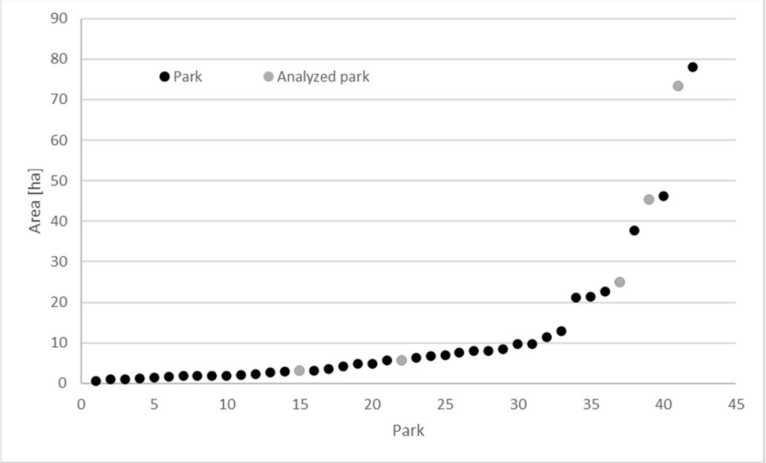

Figure 3. Distribution of urban parks for the city of Wroclaw according to their size. The first two (grey) points denote Park A.

Table 2. Urban park metrics.

Park	Area (ha)	Perimeter (m)	LSI	P_{LC}	Geometry (Not to Scale)
A Park	8.84	1669	1.58	F 7.8% G 71.4% W 7.6% O 13.2%	
B Park	27.57	2845	1.53	F 63.6% G 19.5% W 5.3% O 11.6%	
C Park	45.23	3722	1.43	F 73.2% G 19.3% W 0.0% O 7.5%	
D Park	76.87	6310	2.61	F 92.1% G 7.7% W 0.0% O 0.2%	

Abbreviations: LSI—Landscape Shape Index, P_{LC}—Park Land Cover. Park land cover types: F—Forest, G—Grass, W—Water, O—Other.

Parks with an area of 2 ha or larger were considered in this study only. This is because the size of a single LST map pixel is equal to 900 m^2 or 0.09 ha. This approach has been suggested by other authors, e.g., [13,64]. The average size of all parks in the city is 12.6 ha, whereas the average area of the analysed parks is 39.63 ha. Park metrics have been presented in Table 2. These include: area, perimeter, landscape shape index (LSI) as described in Section 3.3, and proportion of park land cover types including forest, green areas (i.e., grassland, bushes, etc. constituting low and medium sized vegetation), water and other uses such as paths and playgrounds (P_{LC}). Three parks (B, C and D) are predominately covered with high vegetation, with forest areas constituting from 63.6% to 92.1% of their total area. The A Park is dominated by low–medium vegetation (84.6%). Two parks, A and B, have water bodies that cover 7.6% and 5.3% of their area, respectively. Other land uses constitute up to 11.6% of a given park. Three parks (A, B and C) have low LSI index values (1.43 to 1.58) pointing to their generally compact shape, whereas the D Park is more fragmented, with an LSI value of 2.61.

4.2. Spatial Statistics of the Urban Park Effect on LST

The statistics describing the effect of urban parks on the LST distribution and calculated according to the methods stated in Section 3.3 have been presented in Table 3. The values have been calculated for each analysed period, i.e., 2017, 2018 and 2019 independently.

Table 3. Mean park LST and spatial statistics of urban park effect on LST.

Statistics	Park	2017	2018	2019
Mean LST [°C]	A Park	28.2	27.7	28.8
	B Park	25.8	26.7	26.9
	C Park	25.6	25.2	26.3
	D Park	25.7	25.9	26.4
PCA [ha]	A Park	101.6	89.9	78.8
	B Park	199.1	182.4	181.0
	C Park	287.9	312.8	308.3
	D Park	691.8	688.7	660.5
PCE	A Park	11.5	10.2	8.9
	B Park	7.2	6.6	6.6
	C Park	5.3	5.8	5.7
	D Park	9.4	9.4	9.0
PCG [°C/100 m]	A Park	1.3	1.0	1.8
	B Park	1.6	1.2	1.7
	C Park	1.0	0.7	1.0
	D Park	2.1	1.4	2.0
PCI [°C]	A Park	3.1	1.9	2.8
	B Park	3.6	2.1	3.0
	C Park	3.4	2.2	3.0
	D Park	2.9	2.0	2.2
PCIe [°C]	A Park	3.1	2.0	3.0
	B Park	3.6	2.1	3.1
	C Park	3.4	2.3	3.1
	D Park	3.1	2.1	2.3

Abbreviations: LST—Land Surface Temperature, PCA—Park Cooling Area, PCE—Park Cooling Efficiency, PCG—Park Cooling Gradient, PCI—Park Cooling Island, PCIe—Extended Park Cooling Island.

The B, C and D parks have the mean LST in the range of 25.2 °C to 26.9 °C, whereas the mean LST in the smallest A Park ranges from 27.7 °C to 28.8 °C, approximately 2 °C higher. The mean LST is the lowest in the two parks with the largest forest area (parks C and D).

The PCA statistic, i.e., the largest cooling area produced by parks, has been determined for the largest D Park, being on average 660.5 ha to 691.8 ha, and the smallest one for the A Park 78.8 ha to 101.6 ha depending on the year of data acquisition.

In the case of the PCE statistic, i.e., the ratio of the maximum cooling area outside the park to the park area, the lowest values have been determined for the C and B Parks, 5.3 to 5.8 and 6.6 to 7.2, respectively. The highest ratio has been determined for the A Park, 8.9 to 11.5, and the second highest for the D Park. The A Park is the only one surrounded by a densely built-up area from all sides. This indicates that parks influence the temperature on an area approximately five to eleven times that of their size.

The PCG statistic, i.e., the temperature rise per unit of the distance increment (100 m) from the park boundary, has been shown graphically in Figure 4 in the four main geographical directions, as it differs depending on the type of land use in the park's surroundings. The highest values have been obtained for the D Park (1.4 to 2.1 °C/100 m on average), and the lowest for the C Park (0.7 to 1.0 °C/100 m on the average). The A and B parks produced comparable results in the range of 1.0 to 1.8 °C/100 m.

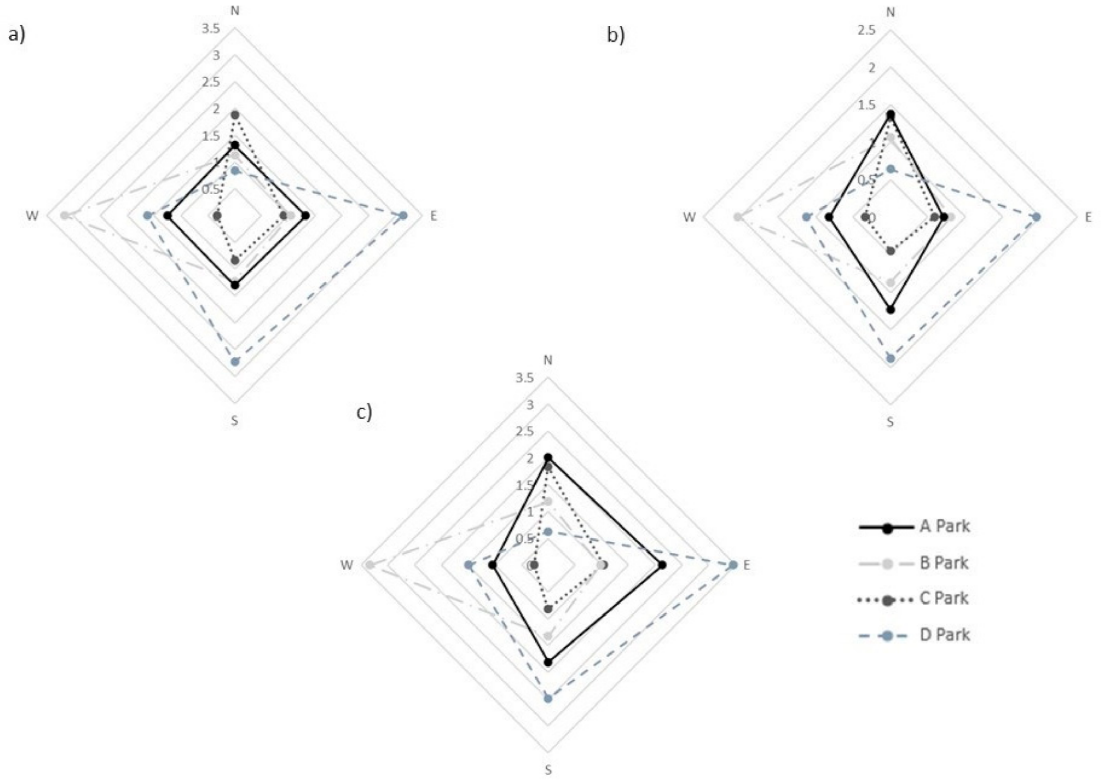

Figure 4. Radar diagrams of park cooling gradient (PCG) (°C/100 m) for (**a**) 2017, (**b**) 2018, and (**c**) 2019.

For the PCI index, representing the difference between the mean LST outside the park in a buffer of 500 m from the park's border and the mean LST inside the park, the values ranged from 1.9 to 3.6 °C. The B and C parks produced the highest PCI values and the A and D parks the lowest. The A Park is surrounded by dense urban development, whereas the D Park by loose urban development and mixed type green areas, which correspond with the obtained values. The B and C parks have mixed type land use in their surroundings and large share of forest, which influences the higher values of the PCI statistic.

For the proposed PCIe statistic, which is the difference between the mean LST outside the park in the buffer zone defined by the maximum cooling range of the park from its border and the mean LST inside the park, the values ranged from 2.0 to 3.6 °C with differences between particular parks in the range of 0.3–0.8 °C.

The range of park influence that determines the PCA shape has been shown in Figure 5 in four main geographical directions. Meanwhile, the graphs of the LST measured from park boundary to edge of the cooling distance, i.e., the distance at which the increase of the LST, as we move away from the park boundary, becomes zero, also known as the first turning point [40,41], have been shown in Figure 6.

4.2.1. A Park

The smallest A Park's cooling effect can be observed from approx. 130 m in the north direction to approx. 325 m in the west direction with the LST difference from 1.9 °C to 5.1 °C depending on the analysed year. The A Park is located in the city centre and is surrounded from all sides predominately by multi-storey residential buildings more densely situated in the north and east parts (Appendix C). The park produced the most uniform spatial picture of PCG. The park's PCA varies from 78.8 ha to 101.6 ha as compared to its size (8.84 ha). This indicates that it has a cooling effect on an area approx. 10 times its size.

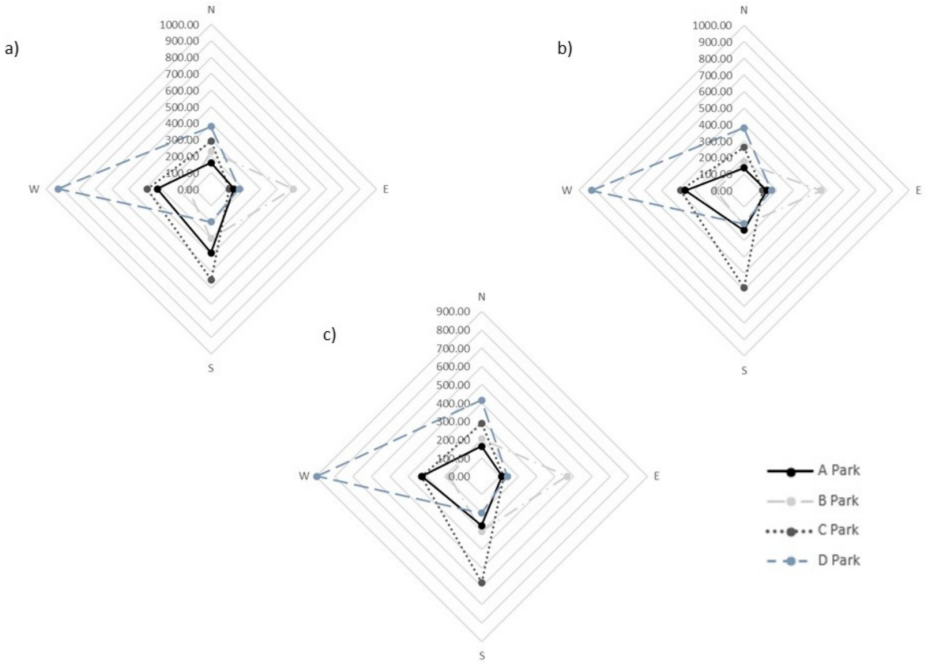

Figure 5. Radar diagrams of the distance (in meters) of the park's cooling influence on surrounding LST for (**a**) 2017, (**b**) 2018, (**c**) 2019.

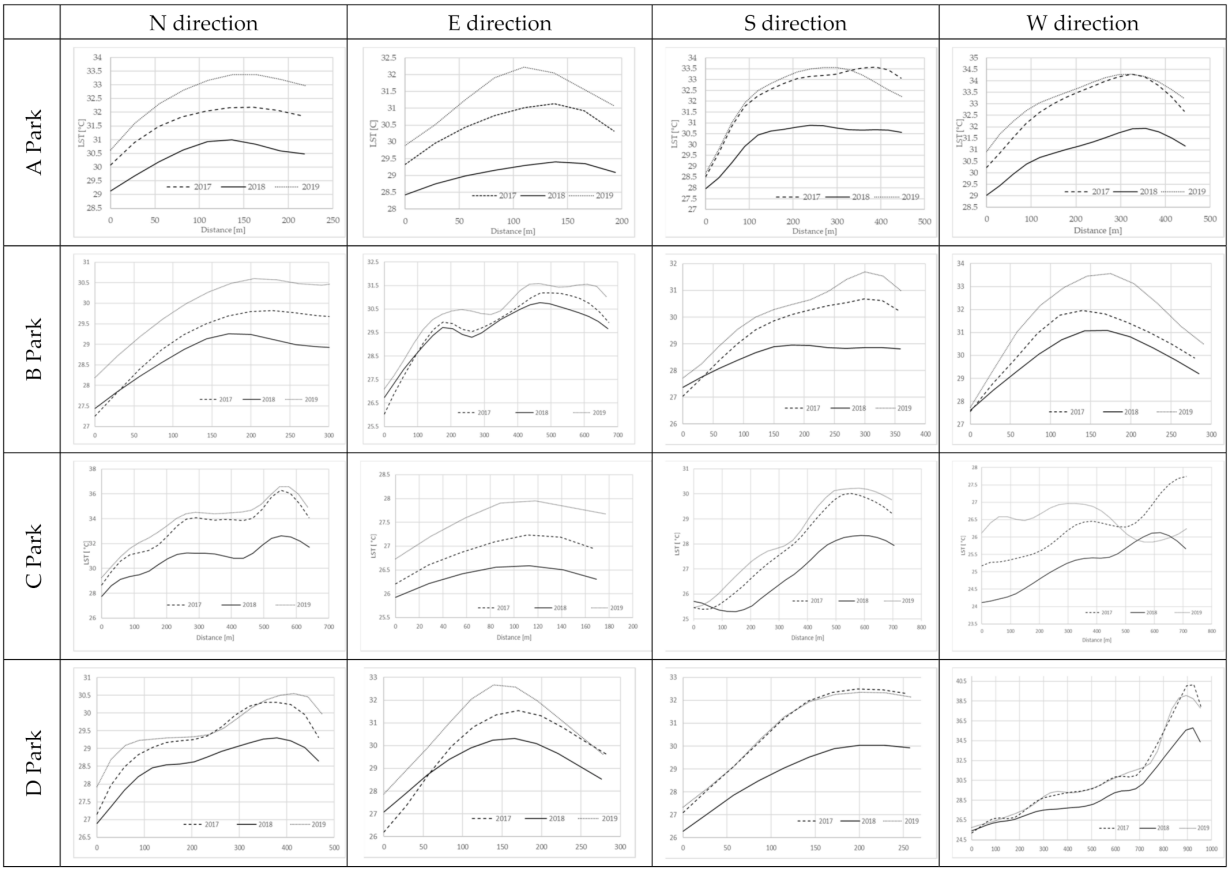

Figure 6. Graphs of LST measured from park boundary to edge of the cooling distance.

4.2.2. B Park

The B Park's cooling effect is from approx. 140–175 m in the west direction to 460–500 m in the east direction with the LST difference from 1.8–2.5 °C/100 to max. 5.8 °C/100 m. The PCG values are up to 3.3 °C in the west direction and lower in the other three directions (1.0 to 1.3 °C). The park is situated in the southern part of the city and its surroundings are characterized by loose urban development on the northern, southern and western sides. In the east, the park is surrounded by single-family housing and industrial and commercial zones. The forest constitutes more than half of its total area (63.6%). The PCA produced by B Park varies from 181 ha to 199 ha.

4.2.3. C Park

The C Park's cooling effect is from approx. 150 m in the east direction to max. 585 m in the south direction, with the LST difference from 0.7–1.2 °C to max. 5.0 °C. The corresponding PCG values range from a low 0.3 °C/100 m to 1.9 °C/100 m. The park is situated in the southern part of the city and the forest makes up 73.2% of its total area. The land use in its surroundings is of mixed type; to the north the park borders with relatively dense residential multi-storey buildings, commercial and industrial areas, to the east with residential zone (mostly semi-detached houses), to the south, first, with low vegetation green spaces, tributary of the Odra River and further away with mixed housing, and to the west with a cemetery (green space) and residential buildings (multi-storey). The PCA produced by this park varies from 287.9 ha to 308.3 ha, whereas its size is 45.23 ha and it has the smallest LSI value of 1.43 (Table 3).

4.2.4. D Park

The D Park's cooling effect is from approx. 130–170 to max. 895–925 m, with the LST difference from 2.4–3.2 °C to as much as 15 °C. The park produces the lowest PCG in the north direction (0.6–0.8 °C/100 m) and the highest, up to 3.4 °C/100 m in the west direction. The D Park is located in the western part of the city and its surroundings are characterized by loose urban development with a small share of commercial and industrial areas and sports grounds in the west. The park is in the vicinity of the Odra River, which flows near the north-east boundary. The area of the park is 75 ha and is mostly covered with forest (92.1%). It is the least compact park, with an LSI index of 2.61 (Table 3). The D Park has the most varied spatial picture of the PCA, with values from 660 ha to 691 ha. This spatial difference may be also caused by the closeness of the Odra River, clearly visible in the picture of the city's LST map.

5. Discussion

Based on the classification of urban park sizes in the city of Wroclaw we have identified four distinct classes and selected one representative park from each class. This is a different approach to those presented in the literature. The other studies range from research of the effect of a single park [11,30,56] through selection of a subset of urban parks based on different criteria [37] to comprehensive studies of all parks in urban area, e.g., [54].

The results show that park characteristics, such as area, shape and forest area, influence the character of the urban park cooling effect. Larger parks are performing better in terms of the cooling efficiency than smaller, compact parks. The same applies to parks with larger forest areas. We have confirmed that the size of forest area in the park increases the cooling distance from the park boundary and the park cooling efficiency, as well as increases the lowering of the LST inside the park. The parks selected for our study are located in different parts of the city and have mixed and different types of land use in their surroundings, ranging from dense urban development to low vegetation and open space. This has also allowed us to analyse the effect of land use type on the cooling efficiency of parks. The cooling efficiency is the lowest for densely built-up residential areas and the highest for open spaces. It should also be noted that the cooling effect of

urban parks may be dependent on the background temperature, which can be nonlinear, as observed in [51,87].

We have used two park metrics to assess the urban park efficiency on lowering the LST, i.e., the LSI, which describes compactness of a given shape and P_{LC} (forest area). There are studies that investigate, e.g., area of water bodies [30,40,50,88] or type of park [40,45]. The other park metrics that can be used include, e.g., area to perimeter ratio [48,55] or more complex indexes such as Fractal Dimension Index, which reflects the extent of shape complexity across a range of spatial scales [89] and has been used in study by [65]. In our study we did not analyse linear parks, such as the one along the city old moat, due to their small sizes (i.e., width). According to the literature, such parks create small LST difference between the park area and its surroundings [54].

Comparison with other studies in comparable geographical and climatic conditions is hindered by the limited number of publications. For example, in the case of [90] the UHI pattern was predominately determined for the city of Leipzig in Germany, whereas in the case of Stockholm (Sweden) [38] ambient air temperature inside one of the parks and in its surroundings were analysed. Our results confirm that, in the case of Wroclaw, located in a temperate continental climate, urban parks produce significant cooling effects. This is in accordance with other studies of cities located in comparable and in different climate zones, e.g., [13,45,48,51,55]. For example, for the city of Changchun (China) located in a cold temperate zone, the strongest PCI was determined for large parks with a cooling extent of approx. 480 m for parks larger than 30 ha [13]. This is comparable with results obtained for medium sized parks (B and C) in Wroclaw. Cao et al. [37] found that the max. PCI intensity was 6.8 degrees for a park size of 41.9 ha in Nagoya (Japan) located in a temperature humid climate, as compared to 3.6 °C in our case. In a study conducted in London (UK), it was determined that the distance over which cooling is experienced increases linearly with increasing green areas. However, the relationships between the amount of cooling and areas are non-linear [51]. Compact and larger forest area lower the park's mean LST and improve the cooling effect; see also [30,44,55]. In our case, the magnitude of this influence and size and shape of PCA differs for each of the analysed parks, as it is determined by park size, forest area, as well as being connected with the type of land use in the vicinity.

These findings have significant implications, as the average temperature in Wroclaw has risen by two degrees in the last few decades. Sustainable urban policy that takes into account the role of parks in regulation of urban temperature may help to mitigate the UHI effect and make it more resilient to the observed climate change.

We have carried out the research for day periods of the highest temperatures. The published studies also indicate that the park cooling efficiency varies depending on the time of the year and between day and night [44,55]. We have used three different datasets (Landsat 8 imagery) acquired during the hottest weather spells in the 2017–2019 period to analyse, repeatedly, the cooling effect of urban parks on the LST in their surroundings. Many publications report studies based on a single satellite dataset only [47,53,54,59], while other ones are based on a set of such images in different configurations, e.g., representing different seasons [13,37] or acquired at monthly intervals [13]. Our observation is that a park cooling island effect should be confirmed by several datasets representing the distribution of the LST.

Analysis of LST distribution based on satellite imagery has the advantage of providing continuous information for the study area in contrast to discrete and usually irregularly spaced ground-based measurements. At the same time, it has limitations set by spatial resolution of the satellite imagery that can reduce the LST retrieval accuracy (land cover product 30 m, water vapor 1 km, TIRS 100 m, and FVC data 30 m) [83]. This eliminates the smallest urban parks from analysis, e.g., [13] suggests that parks smaller than 2 ha should not be considered, whereas [59] included parks larger than 1 ha.

Interpretation of park cooling efficiency and park cooling area should take this aspect into consideration, as the pixel size may lead to value averaging, especially in park boundary zones [37], resulting in a smoother picture of the LST distribution. In general, remotely

sensed data should be accompanied by field measurements of ambient air temperature for reference, however in cases of historical studies it may not be possible to obtain such data. In addition, field measurements are usually limited to point locations or transects. We have applied LST retrieval procedures proposed and successfully used by other authors [82,83]. In future studies, it is better to combine remotely sensed satellite data with in situ observations to examine the cooling effect of urban parks in a more comprehensive way. Additionally, it should be noted that factors such as wind velocity may influence the cooling effect and should be taken into account in future research.

Nonetheless, the advantages of satellite derived LST, such as continuous spatial information and possibility of backward analysis, outweigh these limitations, and it is the most commonly used source of data for LST based studies of urban park cooling effects (Appendix A).

6. Conclusions

This is probably one of the few studies analysing urban park cooling effects on the LST distribution for a medium sized city located in a temperate continental climate, as well as the first study for the city of Wroclaw and foundation for further research. The Wroclaw city has experienced growth of the average ambient air temperature in recent decades, as well as the UHI phenomenon.

We have conducted the study for four parks representative of four distinct classes based on park size. The parks also differ in terms of forest area and location in the city.

This study of the urban park cooling island efficiency has been based on a sequence of LST maps derived from Landsat imagery for three hot weather periods. The land surface temperatures derived from satellite-borne remotely sensed thermal imagery are not the same as ambient air temperatures, and the accuracy of the LST spatial pattern is determined by resolution of the satellite imagery products, which may cause a smoothing effect in the data.

We have determined that the cooling effect of parks varies with park size, forest area, as well as with type of land use in the park surroundings. The cooling distance is the greatest (up to 925 m) for open spaces and the smallest (110–130 m) for densely spaced multi-storey buildings and industrial zones. The average PCG values range from 0.7 to 2.1 °C/100 m, and the PCA values from as low as 78.8 ha (the smallest park surrounded by multi-storey buildings) to 691.8 ha (the largest park with varied land use in its vicinity). Thus, the park cooling effect is heterogenous and differs also with respect to the type of park neighbourhood.

Results of this study have the potential to contribute to the understanding of how urban parks can alleviate the urban heat island phenomenon in continental climate zones. This has significant urban management and planning implications, as sustainable urban development policies that take into account the role of parks in regulation of ambient air temperature may help to mitigate the UHI effect and make the city more resilient to the processes associated with climate change.

Therefore, the findings suggest solutions for urban planners and decision makers facing a developing and modernizing city to choose appropriate sustainable urban strategies by considering locations for new parks and their vegetation composition.

Author Contributions: Conceptualization, J.B.; methodology, J.B.; software, J.B. and M.H.; validation, J.B.; formal analysis, J.B.; investigation, J.B. and M.H.; resources, J.B. and M.H.; data curation, J.B..; writing—original draft preparation, J.B.; writing—review and editing, J.B. and M.H.; visualization, J.B. and M.H.; supervision, J.B.; project administration, J.B. Both authors have read and agreed to the published version of the manuscript. Both authors have read and agreed to the published version of the manuscript.

Funding: This research has been partly supported by the statutory grant at the Department of Geodesy and Geoinformatics, Faculty of Geoengineering, Mining and Geology, Wroclaw University of Science and Technology.

Institutional Review Board Statement: Not applicable.

Informed Consent Statement: Not applicable.

Data Availability Statement: Not applicable.

Conflicts of Interest: The authors declare no conflict of interest.

Appendix A

Table A1. Selected recent studies of urban park cooling effect in chronological order.

Authors (Year of Publication)	Study Type	Source Data	Main Methods	Region, Climate
Jansson et al. (2007) [38]	(1, 2)	Ground based measurements	Temperature difference between the built-up area and the urban park, descriptive statistics	Stockholm (Sweden)/Continental
Cao et al. (2010) [37]	(1, 3)	Aster and Ikonos	Vegetation and shape indexes	Nagoya (Japan)/ Temperate humid
Hamada and Ohta (2010) [42]	(1)	Ground based measurements	Descriptive statistics, bivariate correlation	Nagoya (Japan)/ Temperate humid
Oliveira et al. (2011) [39]	(2)	Ground based measurements	Park cooling intensity (maximum difference between the measured values inside and outside of green area), distance index, influence of the solar exposure	Lisbon (Portugal)/Mediterranean
Mahmoud (2011) [51]	(2, 4)	Ground based measurements, Questionnaire surveys	Thermal comfort indices, regression analysis, descriptive statistics	Cairo (Egypt) /Desert
Cohen et al. (2012) [52]	(4)	Ground based measurements	Physiological Equivalent Temperature, regression analysis, human thermal comfort	Tel Aviv (Israel)/Subtropical Mediterranean
Choi et al. (2012) [43]	(1)	Landsat 7	Kriging, spatial-autocorrelation, inverse distance squared weighting analysis	Seoul (Korea)/Humid continental
Siti Nor Afzan Buyadi et al. (2013) [29]	(4)	Landsat 5	LST transect profiles, Temperature distribution of land use types	Shah Alam, Selangor (Malaysia)/Tropical
Ren et al. (2013) [47]	(3)	Landsat 5, SPOT	Descriptive statistics, correlation of Park Cooling Intensity and forest structure	Changchun, Jilin province (China)/Humid continental with monsoon influence
Kong et al. (2014) [46]	(1, 3)	Landsat 5, Ikonos	Multiple linear regression analysis of vegetation influence on PCI intensity	Nanjing, Jiangsu Province (China)/Subtropical
Chang and Li (2014) [62]	(4)	Ground based measurements	Classification and Regression Tree analysis, regression analysis	Taipei (Taiwan)/Subtropical monsoon
Feyisa et al. (2014) [60]	(1)	Landsat 7, ground based measurements	Park cooling distance, and intensity, regression	Addis Ababa (Ethiopia)/Desert
Skoulika et al. (2014) [11]	(1)	Ground based measurements	Nocturnal and daytime cool island intensity	Athens (Greece)/ Mediterranean
Anjos and Lopes (2014) [61]	(4)	Ground based measurements	Cluster analysis	Aracaju (Brasil)/ Tropical/subtropical
Doick et al. (2014) [44]	(1, 2)	Ground based measurements	Descriptive statistics, distance-temperature ratio, frequency distribution	London (UK)/Temperate oceanic
Cheng et al. (2015) [41]	(1)	Landsat	Correlation of LST and park size	Shanghai, China /Subtropical monsoon
Chen et al. (2015) [56]	(4)	Ground based measurements, Questionnaire surveys	Descriptive statistics, linear regression	Shanghai, China /Subtropical monsoon
Monteiro et al. (2016) [55]	(1, 4)	Ground based measurements	Size metric, regression analysis	London (UK)/Temperate oceanic
Bao et al. (2016) [48]	(1)	Landsat 5, 8	Landscape metrics, park cooling distance and direction	Baotou, Inner Mongolia Province (China)/Continental
Yang et al. (2016) [10]	(1)	Ground based measurements	Diurnal UHI index, frequency distribution of UHI index differences	Beijing (China)/Humid continental
Anguluri and Narayanan (2017) [57]	(4)	Geo-eye	Per capita and proportional green indexes, GIS	Kalaburagi, North Karnataka (India)/ Tropical/subtropical
Du et al. (2017) [59]	(1, 3)	Landsat 8, Google Earth	Green cool indexes: range, amplitude of temperature drop, temperature gradient	Shanghai (China) Subtropical
Park et al. (2017) [45]	(2, 4)	Ground based measurements	Descriptive statistics/ linear regression analysis	Seoul (Korea)/Humid continental climate
Sun et al. (2017) [30]	(4)	Ground based measurements	Relationship between landscape parameters and thermal comfort, Numerical simulation modelling, bivariate regression	Beijing (China)/Humid continental

Table A1. *Cont.*

Authors (Year of Publication)	Study Type	Source Data	Main Methods	Region, Climate
Xu et al. (2017) [49]	(4)	Landsat 5 QuickBird	Landscape structure index, woodland aggregation index, regression analysis	Beijing (China)/Humid continental
Yang et al. (2017) [12]	(3)	Landsat 8,	Area, perimeter, area to perimeter ratio, shape, total area and number of patches metrics	Changchun, Jilin Province (China)/Continental
Yang et al. (2017) [13]	(1, 4)	Landsat 8, GF-2	Urban park metrics (area, perimeter, shape, patch density), cooling effect extent	Changchun/Changchun, Jilin Province (China)/Continental
Yu et al. (2017) [50]	(4)	Landsat 7, 8, SPOT 5,	PCI extent, intensity, efficiency, and TVoE	Fuzhou, Fujian Province (China)/Subtropical
Yu et al. (2018) [28]	(4)	Landsat 7, 8, SPOT 5, Google Earth	Land cover change effect on LST distribution	Fuzhou, Fujian Province (China)/Subtropical
Wang et al. (2018) [54]	(1, 4)	Landsat 8	Temperature Drop Amplitude, Temperature Drop Range, Pearson correlation, regression analysis	Changzhou, Jiangsu Province (China)/Subtropical
Algretawee et al. (2019) [5]	(2)	Ground measurements (handheld devices)	Park cooling magnitude and distance indexes	Melbourne (Australia)/temperate oceanic
Li et al. (2020) [65]	(1, 2, 3)	Landsat 8	Landscape metrics	Zhengzhou (China)/Humid subtropical
Peng et al. (2020) [40]	(1, 3)	Landsat 8	Four park cooling indexes: intensity, gradient, area and efficiency	Shenzen (China)/Subtropical
Qiu and Jia, (2020) [58]	(1)	Landsat 8	PCI range, amplitude of temperature difference, temperature gradient, regression analysis	Beijing (China)/Humid continental

Study types: (1) assessment of park cooling effect, (2) monitoring of park cooling effect, (3) identification of factors influencing park cooling effect], (4) design of parks for increased cooling effect. Abbreviations: LST—land surface temperature, PCI—park cool island, UHI—urban heat island.

Appendix B

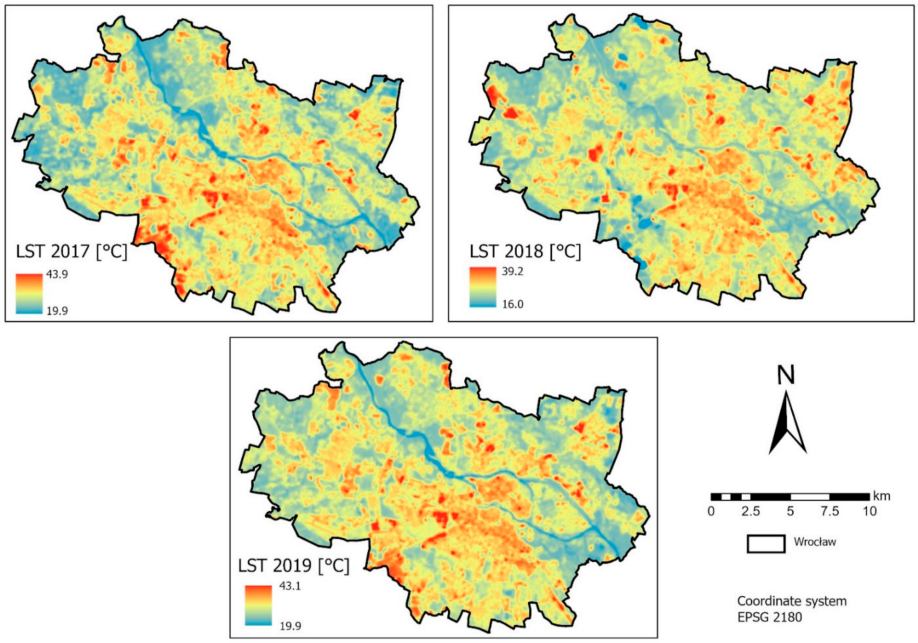

Figure A1. LST maps in Wroclaw for the analysed 2017–2019 periods.

Appendix C

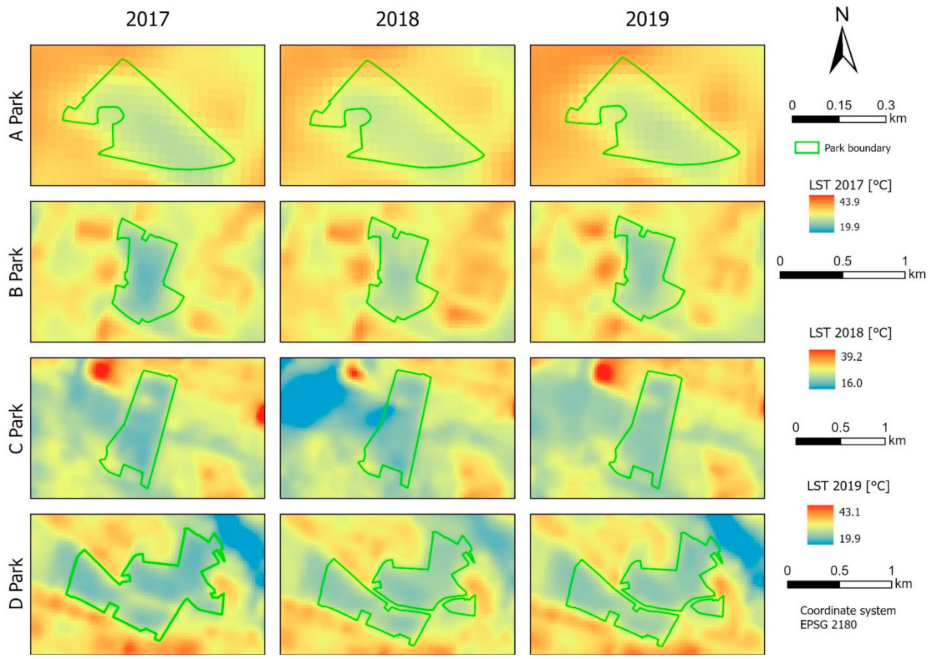

Figure A2. LST maps in the analysed parks.

References

1. Wittig, R.; Sukopp, H. *Was ist Stadtökologie? Stadtökologie*; Gustav Fischer Verlag: Stuttgart, Germany, 1993; pp. 1–9. (In German)
2. Howard, L. *The Climate of London, Deduced from Meteorological Observations, Made at Different Places in the Neighbourhood of the Metropolis, vol. 2, London*; W. Phillips, George Yard, Lombard Street: London, UK, 1818; pp. 1818–1820.
3. Oke, T. Street design and urban canopy layer climate. *Energy Build.* **1988**, *11*, 103–113. [CrossRef]
4. Oke, T.R. The energetic basis of the urban heat island. *Q. J. R. Meteorol. Soc.* **1982**, *108*, 1–24. [CrossRef]
5. Algretawee, H.; Rayburg, S.; Neave, M. Estimating the effect of park proximity to the central of Melbourne city on Urban Heat Island (UHI) relative to Land Surface Temperature (LST). *Ecol. Eng.* **2019**, *138*, 374–390. [CrossRef]
6. Salleh, S.A.; Latif, Z.A.; Mohd, W.M.N.W.; Chan, A. Factors Contributing to the Formation of an Urban Heat Island in Putrajaya, Malaysia. *Procedia-Soc. Behav. Sci.* **2013**, *105*, 840–850. [CrossRef]
7. Wickham, C.; Rohde, R.; Muller, R.A.; Wurtele, J.; Curry, J.; Groom, D.; Jacobsen, R.; Perlmutter, S.; Rosenfeld, A.; Mosher, S. Influence of Urban Heating on the Global Temperature Land Average using Rural Sites Indentifed from MODIS Classifications. *Geoinformat. Geostat.* **2013**. [CrossRef]
8. Dixon, P.G.; Mote, T.L. Patterns and Causes of Atlanta's Urban Heat Island–Initiated Precipitation. *J. Appl. Meteorol. Climatol.* **2003**, *42*, 1273–1284. [CrossRef]
9. Singh, P.; Kikon, N.; Verma, P. Impact of land use change and urbanization on urban heat island in Lucknow city, Central India. A remote sensing based estimate. *Sustain. Cities Soc.* **2017**, *32*, 100–114. [CrossRef]
10. Yang, P.; Xiao, Z.-N.; Ye, M.-S. Cooling effect of urban parks and their relationship with urban heat islands. *Atmos. Ocean. Sci. Lett.* **2016**, *9*, 298–305. [CrossRef]
11. Skoulika, F.; Santamouris, M.; Kolokotsa, D.; Boemi, S.-N. On the thermal characteristics and the mitigation potential of a medium size urban park in Athens, Greece. *Landsc. Urban Plan.* **2014**, *123*, 73–86. [CrossRef]
12. Yang, C.; He, X.; Wang, R.; Yan, F.; Yu, L.; Bu, K.; Yang, J.; Chang, L.; Zhang, S. The Effect of Urban Green Spaces on the Urban Thermal Environment and Its Seasonal Variations. *Forests* **2017**, *8*, 153. [CrossRef]
13. Yang, C.; He, X.; Yu, L.; Yang, J.; Yan, F.; Bu, K.; Chang, L.; Zhang, S. The Cooling Effect of Urban Parks and Its Monthly Variations in a Snow Climate City. *Remote Sens.* **2017**, *9*, 1066. [CrossRef]
14. Unger, J. Intra-urban relationship between surface geometry and urban heat island: Review and new approach. *Clim. Res.* **2004**, *27*, 253–264. [CrossRef]
15. Padhy, S.K.; Sarkar, S.; Panigrahi, M.; Paul, S. Mental health effects of climate change. *Indian J. Occup. Environ. Med.* **2015**, *19*, 3–7. [CrossRef] [PubMed]
16. Yang, T.C.; Jensen, L. Climatic conditions and human mortality: Spatial and regional variation in the United States. *Popul. Environ.* **2017**, *38*, 261–285. [CrossRef] [PubMed]

17. Chiabai, A.; Quiroga, S.; Martinez-Juarez, P.; Higgins, S.; Taylor, T. The nexus between climate change, ecosystem services and human health: Towards a conceptual framework. *Sci. Total Environ.* **2018**, *635*, 1191–1204. [CrossRef] [PubMed]
18. Lou, J.; Wu, Y.; Liu, P.; Kota, S.H.; Huang, L. Health Effects of Climate Change Through Temperature and Air Pollution. *Curr. Pollut. Rep.* **2019**, *5*, 144–158. [CrossRef]
19. Benz, S.A.; Bayer, P.; Goettsche, F.-M.; Olesen, F.S.; Blum, P. Linking Surface Urban Heat Islands with Groundwater Temperatures. *Environ. Sci. Technol.* **2015**, *50*, 70–78. [CrossRef]
20. Zhu, K.; Bayer, P.; Grathwohl, P.; Blum, P. Groundwater temperature evolution in the subsurface urban heat island of Co-logne, Germany. *Hydrol. Process.* **2015**, *29*, 965–978. [CrossRef]
21. Jiang, J.; Tian, G. Analysis of the impact of Land use/Land cover change on Land Surface Temperature with Remote Sensing. *Procedia Environ. Sci.* **2010**, *2*, 571–575. [CrossRef]
22. Xiao, R.-B.; Ouyang, Z.-Y.; Zheng, H.; Li, W.-F.; Schienke, E.W.; Wang, X.-K. Spatial pattern of impervious surfaces and their impacts on land surface temperature in Beijing, China. *J. Environ. Sci.* **2007**, *19*, 250–256. [CrossRef]
23. Howe, D.; Hathaway, J.; Ellis, K.; Mason, L. Spatial and temporal variability of air temperature across urban neighborhoods with varying amounts of tree canopy. *Urban For. Urban Green.* **2017**, *27*, 109–116. [CrossRef]
24. U.S. Environmental Protection Agency. Reducing Urban Heat Islands: Compendium of Strategies. Draft. Available online: https://www.epa.gov/heat-islands/heat-island-compendium (accessed on 26 March 2021).
25. Aram, F.; Garcia, E.H.; Solgi, E.; Mansournia, S. Urban green space cooling effect in cities. *Heliyon* **2019**, *5*, e01339. [CrossRef] [PubMed]
26. Oke, T.R.; Crowther, J.M.; McNaughton, K.G.; Monteith, J.L.; Gardiner, B. The micrometeorology of the urban forest. *Philos. Trans. R. Soc. Lond. B Biol. Sci.* **1989**, *324*, 335–349. [CrossRef]
27. Declet-Barreto, J.; Brazel, A.J.; Martin, C.A.; Chow, W.; Harlan, S.L. Creating the park cool island in an inner-city neighborhood: Heat mitigation strategy for Phoenix, AZ. *Urban Ecosyst.* **2013**, *16*, 617–635. [CrossRef]
28. Yu, Z.; Guo, X.; Zeng, Y.; Koga, M.; Vejre, H. Variations in land surface temperature and cooling efficiency of green space in rapid urbanization: The case of Fuzhou city, China. *Urban For. Urban Green.* **2018**, *29*, 113–121. [CrossRef]
29. Buyadi, S.N.A.; Mohd, W.M.N.W.; Misni, A. Impact of Land Use Changes on the Surface Temperature Distribution of Area Surrounding the National Botanic Garden, Shah Alam. *Procedia-Soc. Behav. Sci.* **2013**, *101*, 516–525. [CrossRef]
30. Sun, S.; Xu, X.; Lao, Z.; Liu, W.; Li, Z.; Garcia, E.H.; He, L.; Zhu, J. Evaluating the impact of urban green space and landscape design parameters on thermal comfort in hot summer by numerical simulation. *Build. Environ.* **2017**, *123*, 277–288. [CrossRef]
31. Sun, Q.; Wu, Z.; Tan, J. The relationship between land surface temperature and land use/land cover in Guangzhou, China. *Environ. Earth Sci.* **2012**, *65*, 1687–1694. [CrossRef]
32. Sun, Q.; Tan, J.; Xu, Y. An ERDAS image processing method for retrieving LST and describing urban heat evolution: A case study in the Pearl River Delta Region in South China. *Environ. Earth Sci.* **2009**, *59*, 1047–1055. [CrossRef]
33. Arulbalaji, P.; Padmalal, D.; Maya, K. Impact of urbanization and land surface temperature changes in a coastal town in Kerala, India. *Environ. Earth Sci.* **2020**, *79*, 1–18. [CrossRef]
34. Jauregui, E. Influence of a large urban park on temperature and convective precipitation in a tropical city. *Energy Build.* **1990**, *15*, 457–463. [CrossRef]
35. Spronken-Smith, R.A.; Oke, T.R.; Lowry, W.P. Advection and the surface energy balance across an irrigated urban park. *Int. J. Climatol.* **2000**, *20*, 1033–1047. [CrossRef]
36. Liu, G.; Zhang, Q.; Li, G.; Doronzo, D.M. Response of land cover types to land surface temperature derived from Landsat-5 TM in Nanjing Metropolitan Region, China. *Environ. Earth Sci.* **2016**, *75*, 1386. [CrossRef]
37. Cao, X.; Onishi, A.; Chen, J.; Imura, H. Quantifying the cool island intensity of urban parks using ASTER and IKONOS data. *Landsc. Urban Plan.* **2010**, *96*, 224–231. [CrossRef]
38. Jansson, C.; Jansson, P.-E.; Gustafsson, D. Near surface climate in an urban vegetated park and its surroundings. *Theor. Appl. Clim.* **2007**, *89*, 185–193. [CrossRef]
39. Oliveira, S.; Andrade, H.; Vaz, T. The cooling effect of green spaces as a contribution to the mitigation of urban heat: A case study in Lisbon. *Build. Environ.* **2011**, *46*, 2186–2194. [CrossRef]
40. Peng, J.; Dan, Y.; Qiao, R.; Liu, Y.; Dong, J.; Wu, J. How to quantify the cooling effect of urban parks? Linking maximum and accumulation perspectives. *Remote Sens. Environ.* **2021**, *252*, 112135. [CrossRef]
41. Cheng, X.; Wei, B.; Chen, G.; Li, J.; Song, C. Influence of Park Size and Its Surrounding Urban Landscape Patterns on the Park Cooling Effect. *J. Urban Plan. Dev.* **2015**, *141*, 4014002. [CrossRef]
42. Hamada, S.; Ohta, T. Seasonal variations in the cooling effect of urban green areas on surrounding urban areas. *Urban For. Urban Green.* **2010**, *9*, 15–24. [CrossRef]
43. Choi, H.-A.; Lee, W.-K.; Byun, W.-H. Determining the Effect of Green Spaces on Urban Heat Distribution Using Satellite Imagery. *Asian J. Atmos. Environ.* **2012**, *6*, 127–135. [CrossRef]
44. Doick, K.J.; Peace, A.; Hutchings, T.R. The role of one large greenspace in mitigating London's nocturnal urban heat island. *Sci. Total Environ.* **2014**, *493*, 662–671. [CrossRef] [PubMed]
45. Park, J.; Kim, J.-H.; Lee, D.K.; Park, C.Y.; Jeong, S.G. The influence of small green space type and structure at the street level on urban heat island mitigation. *Urban For. Urban Green.* **2017**, *21*, 203–212. [CrossRef]

46. Kong, F.; Yin, H.; Wang, C.; Cavan, G.; James, P. A satellite image-based analysis of factors contributing to the green-space cool island intensity on a city scale. *Urban For. Urban Green.* **2014**, *13*, 846–853. [CrossRef]
47. Ren, Z.; He, X.; Zheng, H.; Zhang, D.; Yu, X.; Shen, G.; Guo, R. Estimation of the relationship between urban park characteristics and park cool island intensity by remote sensing data and field measurement. *Forests* **2013**, *4*, 868–886. [CrossRef]
48. Bao, T.; Li, X.; Zhang, J.; Zhang, Y.; Tian, S. Assessing the Distribution of Urban Green Spaces and its Anisotropic Cooling Distance on Urban Heat Island Pattern in Baotou, China. *ISPRS Int. J. Geo-Inf.* **2016**, *5*, 12. [CrossRef]
49. Xu, X.; Cai, H.; Qiao, Z.; Wang, L.; Jin, C.; Ge, Y.; Wang, L.; Xu, F. Impacts of park landscape structure on thermal environment using QuickBird and Landsat images. *Chin. Geogr. Sci.* **2017**, *27*, 818–826. [CrossRef]
50. Yu, Z.; Guo, X.; Jørgensen, G.; Vejre, H. How can urban green spaces be planned for climate adaptation in subtropical cities? *Ecol. Indic.* **2017**, *82*, 152–162. [CrossRef]
51. Mahmoud, A.H.A. Analysis of the microclimatic and human comfort conditions in an urban parkin hot and arid regions. *Build. Environ.* **2011**, *46*, 2641–2656. [CrossRef]
52. Cohen, P.; Potchter, O.; Matzarakis, A. Daily and seasonal climatic conditions of green urban open spaces in the Mediterranean climate and their impact on human comfort. *Build. Environ.* **2012**, *51*, 285–295. [CrossRef]
53. Wang, X.; Cheng, H.; Xi, J.; Yang, G.; Zhao, Y. Relationship between Park Composition, Vegetation Characteristics and Cool Island Effect. *Sustainability* **2018**, *10*, 587. [CrossRef]
54. Wang, G.; Tian, G.; Jombach, S.; Li, H. Mapping and Analyzing the Park Cooling Effect on Urban Heat Island in an Expanding City: A Case Study in Zhengzhou City, China. *Land* **2020**, *9*, 57. [CrossRef]
55. Monteiro, M.V.; Doick, K.J.; Handley, P.; Peace, A. The impact of greenspace size on the extent of local nocturnal air temperature cooling in London. *Urban For. Urban Green.* **2016**, *16*, 160–169. [CrossRef]
56. Chen, L.; Wen, Y.; Zhang, L.; Xiang, W.-N. Studies of thermal comfort and space use in an urban park square in cool and cold seasons in Shanghai. *Build. Environ.* **2015**, *94*, 644–653. [CrossRef]
57. Anguluri, R.; Narayanan, P. Role of green space in urban planning: Outlook towards smart cities. *Urban For. Urban Green.* **2017**, *25*, 58–65. [CrossRef]
58. Qiu, K.; Jia, B. The roles of landscape both inside the park and the surroundings in park cooling effect. *Sustain. Cities Soc.* **2020**, *52*, 101864. [CrossRef]
59. Du, H.; Cai, W.; Xu, Y.; Wang, Z.; Wang, Y.; Cai, Y. Quantifying the cool island effects of urban green spaces using remote sensing Data. *Urban For. Urban Green.* **2017**, *27*, 24–31. [CrossRef]
60. Feyisa, G.L.; Dons, K.; Meilby, H. Efficiency of parks in mitigating urban heat island effect: An example from Addis Ababa. *Landsc. Urban Plan.* **2014**, *123*, 87–95. [CrossRef]
61. Anjos, M.; Lopes, A. Urban Heat Island and Park Cool Island Intensities in the Coastal City of Aracaju, North-Eastern Brazil. *Sustainability* **2017**, *9*, 1379. [CrossRef]
62. Chang, C.-R.; Li, M.-H. Effects of urban parks on the local urban thermal environment. *Urban For. Urban Green.* **2014**, *13*, 672–681. [CrossRef]
63. Honjo, T.; Takakura, T. Analysis of Temperature Distribution of Urban Green Spaces Using Remote Sensing Data. *J. Jpn. Inst. Landsc. Arch.* **1985**, *49*, 299–304. [CrossRef]
64. Hamada, T.; Mikami, T. Cool Island Phenomenon in Urban Green Spaces: A Case Study of Meiji Shrine and Yoyogi Park. *Geogr. Rev. Jpn.* **1994**, *67*, 518–529. [CrossRef]
65. Voogt, J.A.; Oke, T.R. Thermal remote sensing of urban climates. *Remote Sens. Environ.* **2003**, *86*, 370–384. [CrossRef]
66. Statistical Office in Wroclaw. Statistics Poland. Available online: http://demografia.stat.gov.pl/bazademografia/Tables.aspx (accessed on 3 October 2020). (In Polish)
67. Report on the State of the City 2019, Wroclaw City Council. Available online: https://bip.um.wroc.pl/attachments/download/85122 (accessed on 3 October 2020). (In Polish)
68. Szymanowski, M.; Kryza, M. Application of Remotely Sensed Data for Spatial Approximation of Urban Heat Island in the City of Wrocław, Poland. In *JURSE 2011—Joint Urban Remote Sensing Event*; Stilla, U., Gamba, P., Juergens, C., Maktav, D., Eds.; IEEE: Munich, Germany, 2011; pp. 353–356. [CrossRef]
69. Kwiatkowski, J. The range of Sudetes phenomena and their influence on the mesoclimate of the south-western and central regions of Poland. *Pol. Geogr. Rev. Pol.* **1975**, *20*, 1.
70. Sikora, S. *Bioclimate of Wroclaw*; Institute of Geography and Regional Development, University of Wroclaw: Wrocław, Poland, 2008; ISBN 978-83-9281193-2-5.
71. Dubicki, A.; Dubicka, M.; Szymanowski, M. Climate of Wroclaw, Environment. 2002. Available online: http://eko.org.pl/wroclaw/srodowisko/klimat.html (accessed on 3 October 2020). (In Polish)
72. Dąbek, P.B.; Jurasz, J. GIS estimated potential of rooftop PVs in urban areas—Case study Wrocław (Poland). *E3S Web Conf.* **2018**, *45*, 14. [CrossRef]
73. Ogimet Weather Service. Available online: http://ogimet.com/cgi-bin/gsynres?ind=12424&lang=en&decoded=yes&ndays=2&ano=2018&mes=07&day=19&hora=12 (accessed on 2 March 2021).
74. Szymanowski, M.; Kryza, M. Local regression models for spatial interpolation of urban heat island—An example from Wrocław, SW Poland. *Theor. Appl. Clim.* **2011**, *108*, 53–71. [CrossRef]

75. Szymanowski, M. Spatial structure of the urban heat island in Wroclaw, Poland. In Proceedings of the 5th International Conference on Urban Climate, Lodz, Poland, 1–5 September 2003. Available online: http://meteo.geo.uni.lodz.pl/icuc5 (accessed on 15 January 2021).
76. Wroclaw City Council. *Study of the Conditions and Directions of Spatial Development in Wrocław*; Wroclaw City Council: Wroclaw, Poland, 2018. (In Polish)
77. CORINE Land Cover. *Copernicus Land Monitoring Service*; CORINE Land Cover: Copenhagen, Denmark, 2021. Available online: https://land.copernicus.eu/pan-european/corine-land-cover (accessed on 3 May 2021).
78. Head Office of Geodesy and Cartography. National Geodetic and Cartographic Resources. Available online: https://www.geoportal.gov.pl/dane (accessed on 14 December 2020).
79. Wroclaw Spatial Information System. Available online: https://geoportal.wroclaw.pl/en/resources/ (accessed on 15 December 2020).
80. United States Geological Survey. Available online: https://www.usgs.gov/core-science-systems/nli/landsat/using-usgs-landsat-level-1-data-product (accessed on 10 March 2021).
81. ESRI. Available online: https://www.esri.com/en-us/arcgis/products/arcgis-pro/overview (accessed on 11 December 2020).
82. Jin, M.; Li, J.; Wang, C.; Shang, R. A Practical Split-Window Algorithm for Retrieving Land Surface Temperature from Landsat-8 Data and a Case Study of an Urban Area in China. *Remote Sens.* **2015**, *7*, 4371–4390. [CrossRef]
83. Du, C.; Ren, H.; Qin, Q.; Meng, J.; Zhao, S. A Practical Split-Window Algorithm for Estimating Land Surface Temperature from Landsat 8 Data. *Remote Sens.* **2015**, *7*, 647–665. [CrossRef]
84. Avdan, U.; Jovanovska, G. Algorithm for Automated Mapping of Land Surface Temperature Using LANDSAT 8 Satellite Data. *J. Sens.* **2016**, *2016*, 1480307. [CrossRef]
85. Liu, S.; Su, H.; Zhang, R.; Tian, J.; Wang, W. Estimating the Surface Air Temperature by Remote Sensing in Northwest China Using an Improved Advection-Energy Balance for Air Temperature Model. *Adv. Meteorol.* **2016**, *2016*, 1–11. [CrossRef]
86. Wang, C.; Wang, Z.-H.; Wang, C.; Myint, S.W. Environmental cooling provided by urban trees under extreme heat and cold waves in U.S. cities. *Remote Sens. Environ.* **2019**, *227*, 28–43. [CrossRef]
87. Suchecka, J. Spatial statistics. Methods of analyzing spatial structures. *Procedia Soc. Behav. Sci.* **2014**, *21*, 43–52. (In Polish)
88. Cai, Z.; Han, G.; Chen, M. Do water bodies play an important role in the relationship between urban form and land surface temperature? *Sustain. Cities Soc.* **2018**, *39*, 487–498. [CrossRef]
89. Leitao, A.B.; Miller, J.; Ahern, J.; McGarigal, K. *Measuring Landscapes: A Planner's Hand-Book*; Island Press: Washington, DC, USA, 2012; ISBN 978-1-59726-772-4.
90. Schwarz, N.; Schlink, U.; Franck, U.; Großmann, K. Relationship of land surface and air temperatures and its implications for quantifying urban heat island indicators—An application for the city of Leipzig (Germany). *Ecol. Indic.* **2012**, *18*, 693–704. [CrossRef]